Enhanced Kerr nonlinearity in a left-handed three-level atomic system driven by a bichromatic field*

Yang Xiao-Yu(杨晓雨)[a] and Jiang Yong-Yuan(姜永远)[a)b)†]

[a] Department of Physics, Harbin Institute of Technology, Harbin 150001, China
[b] Key Lab of Micro-Optics and Photonic Technology of Heilongjiang Province, Harbin 150001, China

(Received 13 April 2013; revised manuscript received 20 May 2013)

Enhanced Kerr nonlinearity in a left-handed atomic system consisting of three levels driven by a bichromatic field is presented in this paper. Based on bichromatic field coherence, the real parts of the permittivity and permeability can obtain negative values simultaneously in the same detuning frequency region. By adjusting the frequency difference and the Rabi frequencies of the bichromatic field, the multi-band left-handed behavior of the presented atomic metamaterial is exhibited. Meanwhile, the enhanced Kerr nonlinearity can be realized in this multi-band left-handed three-level atomic system. It is shown that the third-order susceptibility possesses focusing or defocusing properties in the same frequency band.

Keywords: left-handed, Kerr nonlinearity, bichromatic field, multi-band

PACS: 42.50.Gy, 42.25.Bs, 42.65.An, 78.20.Ci **DOI:** 10.1088/1674-1056/22/11/114204

1. Introduction

In recent years, the search for left-handed materials (LHMs)[1] within their supervising and counterintuitive electromagnetic properties has attracted a considerable amount of interest. Experimentally, left-handedness has been realized with the methods of artificial composite metamaterials,[2–4] photonic crystal structures,[5,6] transmission line simulation[7] and chiral media.[8,9] These methods can be observed in the microwave band based on classical electromagnetic theory. Recently, the photonic resonant method based on quantum interference and coherence was first used to theoretically realize the left-handedness in a three-level atomic system by Oketl and Müstecaplioğlu in 2004.[10] As proposed in that paper, the real parts of both the permeability and permittivity could simultaneously obtain negative values over a certain frequency band under the condition of electromagnetically induced transparency (EIT) and the local field effect. This quantum optics method has many attractive advantages compared with classical electromagnetic method, such as realizing negative refraction in the optical regime, requiring no delicate fabrication of spatially periodic structure, being suitable for isotropic media, achieving low, even zero, absorption, etc.[11–20,30,31] It is found that the scheme proposed in the quantum optic method is the atomic system driven by a monochromatic resonant field and the system that is usually comprised of multiple atomic levels interacting with the external fields will increase the number of uncontrollable parameters of the atomic system. For this reason, the atomic system becomes very unstable.

Dual-band of negative refractive index in the atomic system in an optic frequency range was first presented in Ref. [20]. In that work, a four-level atomic system with three external fields was considered. However, the numbers of atomic levels involved in the interaction are too large, which makes the system unstable. Dual-band left-handedness is restricted by the number of atomic levels. Moreover that scheme introduces more uncontrollable parameters. In this paper, we propose a Λ-type three-level atomic system driven by a bichromatic field.[21–24] It can be found that the controllable parameters of the atomic system are increased and the stability of the atomic system is enhanced due to the introduced bichromatic field. The bichromatic field interacts with the atomic levels, which induces multi-level splitting in this atomic system. It stimulates atomic transition between the splitting levels and causes the atomic system to produce multi-channel quantum interference. Multi-band left-handedness can be realized in our atomic system due to multi-channel quantum interference. We are also concerned about the nonlinearity of a left-handed atomic system driven by bichromatic field. However, nonlinear effect in LHM has not been extensively studied in theory in the past. Kerr nonlinearity accompanied by vanishing absorption was first analyzed in a left-handed four-level atomic system by Zhang *et al.*[25] The third-order susceptibility $\mathrm{Re}[\chi^{(3)}]$ in that proposed atomic system increases nine orders compared with in the conventional system. Then, in our proposed Λ-type three-level atomic scheme coupled with a bichromatic field, Kerr nonlinearity can be enhanced by two orders compared with that reported in Ref. [25]. Furthermore, it can be found that the third-order susceptibility shows focusing or defocusing properties in the same left-handed frequency band.

*Project supported by the National Natural Science Foundation of China (Grant Nos. 50836002 and 51176041) and the National Basic Research Program of China (Grant No. 2013CB328702).

†Corresponding author. E-mail: jiangyy@hit.edu.cn

© 2013 Chinese Physical Society and IOP Publishing Ltd

2. Physical model

Consider a lambda-type three-level atomic system as shown in Fig. 1. It has the following properties: upper level $|3\rangle$ and low level $|1\rangle$ have opposite parities and $\boldsymbol{d}_{13} = \langle 1|\hat{\boldsymbol{d}}|3\rangle \neq 0$, where $\hat{\boldsymbol{d}}$ is the electric dipole operator; levels $|1\rangle$ and $|3\rangle$ have the same parities and $\boldsymbol{\mu}_{12} = \langle 1|\hat{\boldsymbol{\mu}}|2\rangle \neq 0$, with $\hat{\boldsymbol{\mu}}$ being the magnetic dipole operator. The bichromatic coupling field $E(t) = \frac{1}{2}(E_{c1} + E_{c2}\,e^{i\delta t})\,e^{-i\omega_{c1}t} + \text{c.c.}$ shows level $|2\rangle$ coupled to level $|3\rangle$, where E_{c1} and E_{c2} are amplitudes, ω_{c1} and ω_{c2} are the frequencies of the bichromatic field. A weak probe field Ω_p with frequency ω_p is used to probe the transition from $|1\rangle$ to $|3\rangle$.

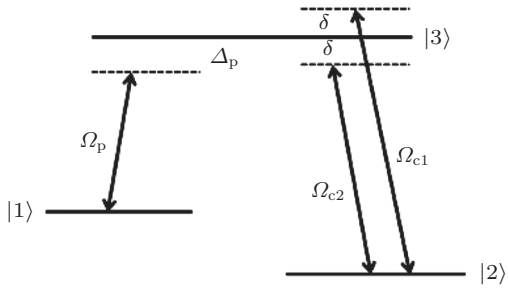


Fig. 1. Schematic of a three-level atomic system interacting with a bichromatic coupled field and a weak probe field.

In the interaction representation, the Hamiltonian under the electric-dipole approximation and rotating-wave approximation can be written as

$$\begin{aligned} H &= -\hbar[\Delta_p\,|3\rangle\langle 3| + (\Delta_p - \Delta_c)\,|2\rangle\langle 2|] - \frac{\hbar}{2}(\Omega_p\,|3\rangle\langle 1| \\ &\quad + (\Omega_{c1} + \Omega_{c2}\,e^{-i\delta t})\,|3\rangle\langle 2|) + \text{H.c.}, \end{aligned} \tag{1}$$

where $\delta = (\omega_1 - \omega_2)/2$ is the frequency difference between the bichromatic fields, $\Delta_c = \Delta_{c1} - \delta$, H.c. represents the interaction of the dual operator Hermitian conjugate terms. The Rabi frequencies of these three optical fields are $\Omega_{c1} = \boldsymbol{E}_{c1}\cdot\boldsymbol{d}_{23}/\hbar$, $\Omega_{c2} = \boldsymbol{E}_{c2}\cdot\boldsymbol{d}_{23}/\hbar$, and $\Omega_p = \boldsymbol{E}_p\cdot\boldsymbol{d}_{13}/\hbar$, respectively d_{23} and d_{13} are the atomic transition electric dipole moments, $\Delta_p = \omega_{31} - \omega_p$ and $\Delta_{c1} = \omega_{32} - \omega_{c1}$ denote the detunings of the probe and bichromatic field, respectively, $\omega_{ij} = \omega_i - \omega_j$ is the atomic resonant transition frequency of levels $|i\rangle$ and $|j\rangle$ $(i, j = 1, 2, 3)$.

Using the Liouville equation for the motion of density operator and spontaneous emission, the Bloch equations for density matrix elements are in the forms of

$$\begin{aligned} \frac{\partial\rho_{11}}{\partial t} &= \gamma_1\rho_{33} + \frac{i}{2}\Omega_p\rho_{31} - \frac{i}{2}\Omega_p\rho_{13}, \\ \frac{\partial\rho_{22}}{\partial t} &= \gamma_2\rho_{33} + \frac{i}{2}(\Omega_{c1} + \Omega_{c2}\,e^{i\delta t})\rho_{32} \\ &\quad - \frac{i}{2}(\Omega_{c1} + \Omega_{c2}\,e^{-i\delta t})\rho_{23}, \\ \frac{\partial\rho_{12}}{\partial t} &= -\gamma_{12}\rho_{12} + \frac{i}{2}(\Omega_{c1} + \Omega_{c2}\,e^{-i\delta t})\rho_{32} - \frac{i}{2}\Omega_p\rho_{32}, \\ \frac{\partial\rho_{13}}{\partial t} &= -\gamma_{13}\rho_{13} + \frac{i}{2}\Omega_p(1 - 2\rho_{11} - \rho_{22}) \\ &\quad - \frac{i}{2}(\Omega_{c1} + \Omega_{c2}\,e^{i\delta t})\rho_{12}, \\ \frac{\partial\rho_{23}}{\partial t} &= -\gamma_{23}\rho_{23} + \frac{i}{2}(\Omega_{c1} + \Omega_{c2}\,e^{i\delta t}) \\ &\quad \times (1 - 2\rho_{22} - \rho_{11}) + \frac{i}{2}\Omega_p\rho_{21}. \end{aligned} \tag{2}$$

Equations obey the conditions: $\rho_{ij} = \rho_{ji}^*$ and $\sum_{i=1}^{4}\rho_{ii} = 1$. Here, γ_1 and γ_2 are the atomic decays. The parameters in Eq. (2) are defined as

$$\begin{aligned} \gamma_{12} &= \gamma_{21}^* = i(\Delta_p - \Delta_{c1}), \\ \gamma_{13} &= \gamma_{31}^* = \frac{\gamma_1 + \gamma_2}{2} + i\Delta_p, \\ \gamma_{23} &= \gamma_{32}^* = \frac{\gamma_1 + \gamma_2}{2} + i\Delta_{c1}. \end{aligned} \tag{3}$$

In order to solve Eq. (2), we will take the same techniques as those in Refs. [23] and [26]. The harmonic expansion method will be used and the density matrix elements are expanded into

$$\rho_{ij} = \sum_{n=-\infty}^{+\infty}\rho_{ij}^{(n)}\,e^{in\delta t}, \quad (i, j = 1, 2, 3), \tag{4}$$

where $\rho_{ij}^{(n)}\,e^{in\delta t}$ is the slowly varying amplitude and n is an integer that varies from $-\infty$ to ∞. Then, we substitute Eq. (4) into Eq. (2) and the complex conjugate of the non-diagonal element leads to an infinite set of equations. The steady-state solutions can be solved by the method of matrix inversion. To do this, an $8\times(2N+1)$ column vector $\boldsymbol{X}$ can be constructed as

$$\begin{aligned} \boldsymbol{X} &= (X_1^{(-N)}, \ldots, X_8^{(-N)}; \ldots; X_1^{(0)}, \ldots, X_8^{(0)}; \ldots; \\ &\quad X_1^{(N)}, \ldots, X_8^{(N)})^T, \\ l &= -N \ldots 0 \ldots N, \end{aligned} \tag{5}$$

$$X_{1-8}^{(n)} = (\rho_{31}^{(n)}, \rho_{13}^{(n)}, \rho_{21}^{(n)}, \rho_{12}^{(n)}, \rho_{32}^{(n)}, \rho_{23}^{(n)}, \rho_{11}^{(n)}, \rho_{22}^{(n)})^T, \tag{6}$$

where the value of the integer N is chosen appropriately to determine the dimension of the vector $\boldsymbol{X}$. Equation (2) can be written in the form of

$$\frac{d\boldsymbol{X}}{dt} + \boldsymbol{Q}\boldsymbol{X} = \boldsymbol{R}. \tag{7}$$

Equation (17) is solved in the steady state form by setting the time derivatives to be zero and using matrix frame inversion as

$$\boldsymbol{X} = -\boldsymbol{Q}^{-1}\boldsymbol{R}, \tag{8}$$

where $\boldsymbol{Q}$ is an $[8\times(2N+1)]\times[8\times(2N+1)]$ tridiagonal matrix, i.e.,

$$\boldsymbol{Q}=\begin{bmatrix} B_{-N} & C & & & & & & & & & \\ A & B_{-N+1} & C & & & & & & & & \\ & \ddots & \ddots & \ddots & & & & & & & \\ & & & A & B_{-1} & C & & & & & \\ & & & & A & B_0 & C & & & & \\ & & & & & \ddots & \ddots & \ddots & & & \\ & & & & & & & A & B_{N-1} & C & \\ & & & & & & & & A & B_N \end{bmatrix}, \tag{9}$$

$$\boldsymbol{A}=\begin{bmatrix} 0 & 0 & 0 & 0 & 0 & 0 & 0 & 0 \\ 0 & 0 & 0 & \frac{\mathrm{i}}{2}\Omega_{\mathrm{c}2} & 0 & 0 & 0 & 0 \\ -\frac{\mathrm{i}}{2}\Omega_{\mathrm{c}2} & 0 & 0 & 0 & 0 & 0 & 0 & 0 \\ 0 & 0 & 0 & 0 & 0 & 0 & 0 & 0 \\ 0 & 0 & 0 & 0 & 0 & 0 & 0 & 0 \\ 0 & 0 & 0 & 0 & 0 & 0 & \frac{\mathrm{i}}{2}\Omega_{\mathrm{c}2} & \mathrm{i}\Omega_{\mathrm{c}2} \\ 0 & 0 & 0 & 0 & 0 & 0 & 0 & 0 \\ 0 & 0 & 0 & 0 & -\frac{\mathrm{i}}{2}\Omega_{\mathrm{c}2} & 0 & 0 & 0 \end{bmatrix}, \tag{10}$$

$$\boldsymbol{B}=\mathrm{i}n\delta I+\begin{bmatrix} \gamma_{31} & 0 & -\frac{\mathrm{i}}{2}\Omega_{\mathrm{c}1} & 0 & 0 & 0 & -\mathrm{i}\Omega_{\mathrm{p}} & -\frac{\mathrm{i}}{2}\Omega_{\mathrm{p}} \\ 0 & \gamma_{13} & 0 & \frac{\mathrm{i}}{2}\Omega_{\mathrm{c}1} & 0 & 0 & \mathrm{i}\Omega_{\mathrm{p}} & \frac{\mathrm{i}}{2}\Omega_{\mathrm{p}} \\ -\frac{\mathrm{i}}{2}\Omega_{\mathrm{c}1} & 0 & \gamma_{21} & 0 & 0 & \frac{\mathrm{i}}{2}\Omega_{\mathrm{p}} & 0 & 0 \\ \frac{\mathrm{i}}{2}\Omega_{\mathrm{c}1} & 0 & 0 & \gamma_{12} & -\frac{\mathrm{i}}{2}\Omega_{\mathrm{p}} & 0 & 0 & 0 \\ 0 & 0 & 0 & -\frac{\mathrm{i}}{2}\Omega_{\mathrm{p}} & \gamma_{32} & 0 & -\frac{\mathrm{i}}{2}\Omega_{\mathrm{c}1} & -\mathrm{i}\Omega_{\mathrm{c}1} \\ 0 & 0 & \frac{\mathrm{i}}{2}\Omega_{\mathrm{p}} & 0 & 0 & \gamma_{23} & \frac{\mathrm{i}}{2}\Omega_{\mathrm{c}1} & \mathrm{i}\Omega_{\mathrm{c}1} \\ -\frac{\mathrm{i}}{2}\Omega_{\mathrm{p}} & \frac{\mathrm{i}}{2}\Omega_{\mathrm{p}} & 0 & 0 & 0 & 0 & \gamma_1 & \gamma_1 \\ 0 & 0 & 0 & 0 & -\frac{\mathrm{i}}{2}\Omega_{\mathrm{c}1} & \frac{\mathrm{i}}{2}\Omega_{\mathrm{c}1} & \gamma_2 & \gamma_2 \end{bmatrix}, \tag{11}$$

$$\boldsymbol{C}=\begin{bmatrix} 0 & 0 & -\frac{\mathrm{i}}{2}\Omega_{\mathrm{c}2} & 0 & 0 & 0 & 0 & 0 \\ 0 & 0 & 0 & 0 & 0 & 0 & 0 & 0 \\ 0 & 0 & 0 & 0 & 0 & 0 & 0 & 0 \\ 0 & \frac{\mathrm{i}}{2}\Omega_{\mathrm{c}2} & 0 & 0 & 0 & 0 & 0 & 0 \\ 0 & 0 & 0 & 0 & 0 & 0 & -\frac{\mathrm{i}}{2}\Omega_{\mathrm{c}2} & -\mathrm{i}\Omega_{\mathrm{c}2} \\ 0 & 0 & 0 & 0 & 0 & 0 & 0 & 0 \\ 0 & 0 & 0 & 0 & 0 & 0 & 0 & 0 \\ 0 & 0 & 0 & 0 & \frac{\mathrm{i}}{2}\Omega_{\mathrm{c}2} & 0 & 0 & 0 \end{bmatrix}, \tag{12}$$

$\boldsymbol{R}$ is an $8\times(2N+1)$ column vector, i.e.,

$$\boldsymbol{R}=(R_1^{-N},\ldots,R_8^{-N};\ldots;R_1^0,\ldots,R_8^0;\ldots;R_1^N,\ldots,R_8^N)^{\mathrm{T}}, \tag{13}$$

with non-zero matrix elements being

$$\begin{aligned} &R_1^{(0)}=-\frac{\mathrm{i}}{2}\Omega_{\mathrm{p}},\quad R_2^{(0)}=\frac{\mathrm{i}}{2}\Omega_{\mathrm{p}},\quad R_5^{(0)}=-\frac{\mathrm{i}}{2}\Omega_{\mathrm{c}1},\\ &R_6^{(0)}=\frac{\mathrm{i}}{2}\Omega_{\mathrm{c}1},\quad R_7^{(0)}=\gamma_1,\quad R_8^{(0)}=\gamma_2,\\ &R_5^{(-1)}=-\frac{\mathrm{i}}{2}\Omega_{\mathrm{c}2},\quad R_6^{(1)}=\frac{\mathrm{i}}{2}\Omega_{\mathrm{c}2}. \end{aligned} \tag{14}$$

The density matrix elements of arbitrary order of this atomic system can be obtained by substituting expressions (9)–(14) into Eq. (18). As shown, the resulting equation is our final formula expressing the optical Bloch equation for a three-level atom coupled by a bichromatic field.

The electric response and magnetic response of our atomic system to the probe field depend on the steady-state values of the one-order coherence terms $\rho_{31}^{(1)}$ and $\rho_{21}^{(1)}$, respectively. For simplicity, the atomic polarizability tensor becomes a scalar as[20]

$$\alpha_{\mathrm{e}}=\frac{d_{13}\rho_{31}^{(1)}}{\varepsilon_0 E_{\mathrm{p}}}, \tag{15}$$

and magnetic susceptibilities can be written as[16–20]

$$\alpha_{\mathrm{m}}=\frac{c\mu_0|\mu_{12}||d_{13}|\rho_{21}^{(1)}}{\eta\hbar\Omega_{\mathrm{p}}}, \tag{16}$$

where ε_0 and μ_0 are the permittivity and permeability of a vacuum, respectively; c is the speed of light in a vacuum; $\eta=1$ is a unitary complex number. In our atomic system, the

atomic density of dense gas is assumed to be $N' = 10^{25}$ m^{-3}. In this dense medium, closely packed atoms give rise to the internal field. The local fields will enhance and maintain a large enough magnetization. With the help of the local fields, the permeability of the atomic medium can have negative value more easily than in nature. According to the Clausius–Mossotti relation,[27,28] the one-order relative permittivity and one-order relative permeability are as follows:

$$\varepsilon_{\rm r} = \frac{1+2N'\alpha_{\rm e}/3}{1-N'\alpha_{\rm e}/3}, \tag{17}$$

$$\mu_{\rm r} = \frac{1+2N'\alpha_{\rm m}/3}{1-N'\alpha_{\rm m}/3}. \tag{18}$$

In order to analyze Kerr nonlinearity of our atomic system, we will consider the third-order susceptibility. According to Ref. [25], the expression of third-order susceptibility is written as

$$\chi^{(3)} = \frac{N'|d_{13}|^4 \rho_{31}^{(3)}}{\varepsilon_0 \hbar^3 |\Omega_{\rm p}|^2 \Omega_{\rm p}}, \tag{19}$$

where $\rho_{31}^{(3)}$ is the third-order coherent term. Up to now, we have obtained all the expressions for the permittivity, permeability and third-order susceptibility of this atomic system. In this paper, the general forms of the relevant off-diagonal elements are very tedious; for this reason, we will present the numerical analysis to the system of three-level atomic interacting with bichromatic fields subsequently.

3. Numerical analysis

In the case of the bichromatic field, the response of the atomic system is less related to the phase of the bichromatic field and it mainly depends on oscillation amplitudes of and frequency difference between bichromatic fields. In the following, we will numerically analyze the electromagnetic properties of our atomic system by varying the frequency difference δ and the Rabi frequencies of the bichromatic field $\Omega_{\rm c1}$ and $\Omega_{\rm c2}$. Oktel and Müstecaplioğlu[10] suggested that the left-handedness be realized in a dense gas of ^{23}Na atoms. We adopt the same Λ type atomic system, and the atomic density $N' = 10^{25}$ m^{-3}. The Rabi frequency of the weak probe field is $\Omega_{\rm p} = 0.01\gamma$. For simplicity, we set one of the detuning frequencies of the bichromatic field to be $\Delta_{\rm c1} = \delta$.

Figures 2(a)–2(d) show the values? permittivity and the permeability versus $\Delta_{\rm p}$ with $\Omega_{\rm c1} = \Omega_{\rm c2} = 3.8\gamma$, $\delta = 4\gamma$. As is well known, an important feature of the left-handed materials is that the real parts of the permittivity and the permeability can simultaneously obtain negative values over a certain frequency band. From Figs. 2(a) and 2(c), it can be seen that the real parts of the permittivity and the permeability can simultaneously obtain negative values over certain frequency bands in three different parts (plotted in the gray areas). Therefore, left-handedness can be realized in these three discontinuous intervals. In the range of $\Delta_{\rm p} < 0$, there is only one left-handed interval, and in the range of $\Delta_{\rm p} > 0$, it has two intervals to realize the left-handed feature. Figures 2(b) and 2(d) show the curves of imaginary parts of $\varepsilon_{\rm r}$ and $\mu_{\rm r}$ versus probe detuning. As exhibited in Fig. 2(b), the imaginary part of the permittivity can obtain very small values in three gray intervals. It will enhance the resonance phenomena and reduce the absorption of the probe field which can store energy of the atomic system. This feature has great significance for realizing left-handedness.

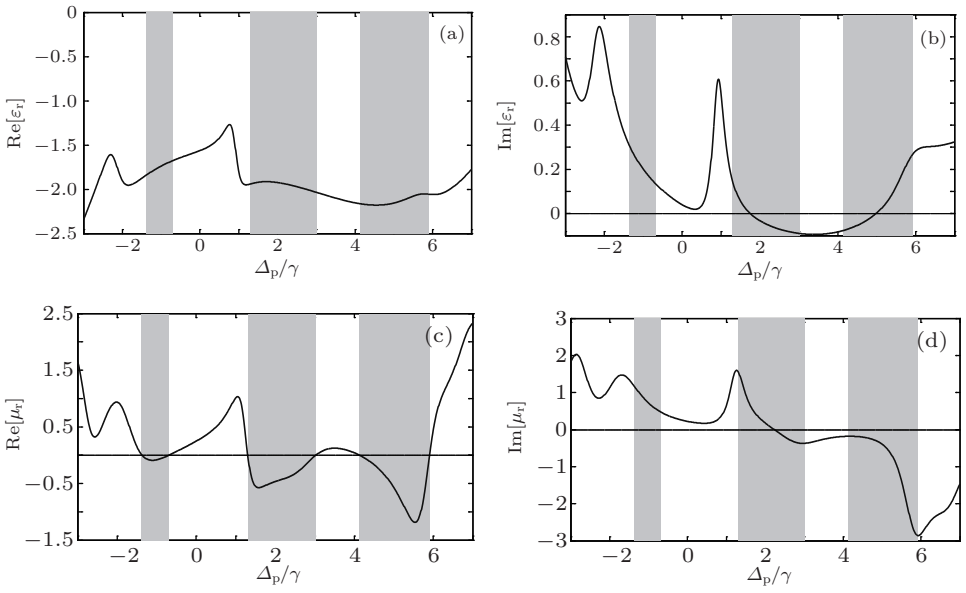


Fig. 2. Curves of real (a) and imaginary (b) parts of $\varepsilon_{\rm r}$ and real (c) and imaginary (d) parts of $\mu_{\rm r}$ versus probe detuning $\Delta_{\rm p}$, for values of the bichromatic field: $\Omega_{\rm c1} = \Omega_{\rm c2} = 3.8\gamma$, $\delta = 4\gamma$. The left-handed properties are indicated in gray regions.

In Figs. 2(a)–2(d), it is found that ε_r and μ_r have three values in different frequency regions. The reason is that the strong bichromatic field interacts with the transition from levels $|3\rangle$ to $|2\rangle$, and the two levels are equidistantly split into multi-levels as the interpretation of the dressed states.[14] The field coherence is greatly enhanced due to multi-quantum channel transition induced by the strong bichromatic field. The weak probe field scans the splitting energy levels and level $|1\rangle$. The electric-dipole transition (between $|1\rangle$ and $|3\rangle$) and the magnetic–dipole transition (between $|1\rangle$ and $|2\rangle$) produce the electric polarizability and the magnetic susceptibility, which are greatly enhanced, respectively.

We have analyzed the linear effects of this left-handed atomic system coupled by a bichromatic field in the foregoing section. Next, we will focus on the nonlinear effect of this left-handed atomic system. As shown in Figs. 3(a), 3(c), and 3(e), the real parts of the third-order susceptibility have different features in left-handed frequency bands. As is well known, the focusing and defocusing effects will be controlled by changing the sign of $\mathrm{Re}[\chi_e^{(3)}]$. When $\mathrm{Re}[\chi_e^{(3)}] > 0$, the focusing effect occurs; the defocusing effect will occur when $\mathrm{Re}[\chi_e^{(3)}] < 0$. From Figs. 3(a), 3(c), and 3(e), we find that only one defocusing effect takes place in the first left-handed frequency band; while the focusing effect and the defocusing effect occur in the other two left-handed frequency bands.

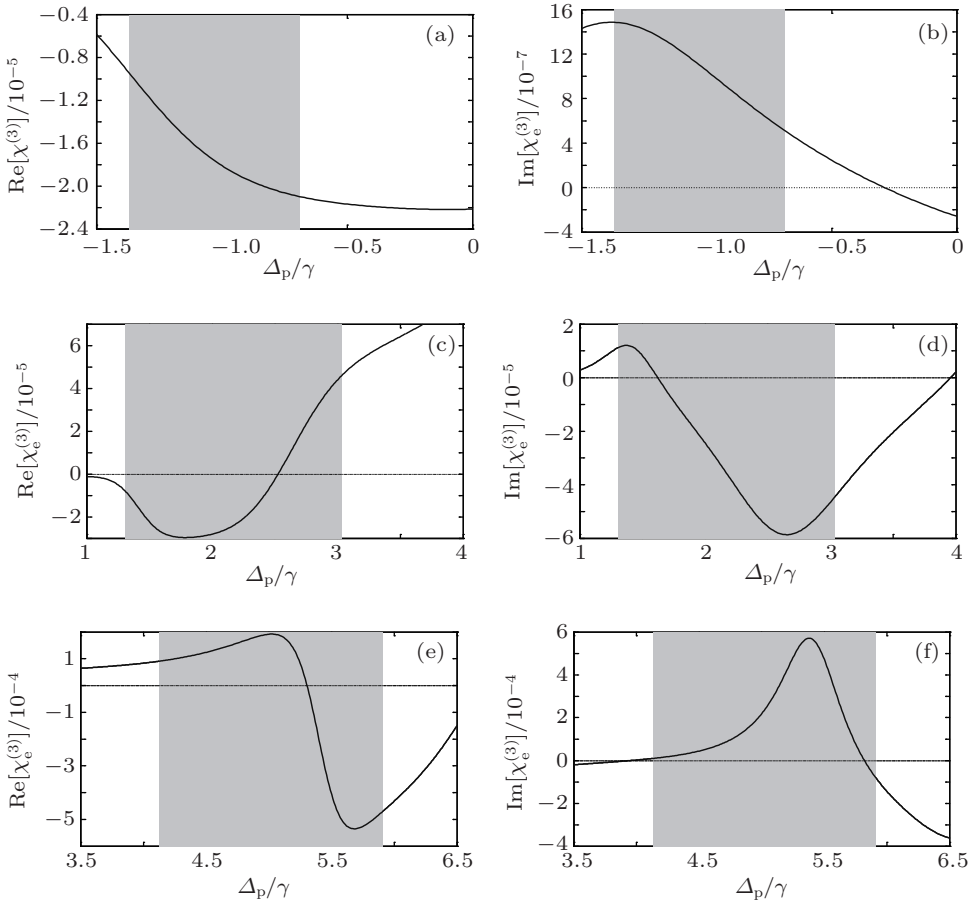


Fig. 3. Curves of real parts of the third-order nonlinearity $\chi_e^{(3)}$ (panels (a), (c), and (e)), and imaginary parts of the third-order nonlinearity $\chi_e^{(3)}$ (panels (b), (d), and (f)) versus probe detuning Δ_p. The three discontinuous left-handed ranges are indicated in the gray regions. The parameters are the same as those in Fig. 2.

As plotted in Figs. 3(c) and 3(e), $\mathrm{Re}[\chi_e^{(3)}]$ changes its sign at $\Delta_p \approx 2.5\gamma$ and $\Delta_p \approx 5.4\gamma$, respectively. In Fig. 3(c), the third-order nonlinearity $\mathrm{Re}[\chi_e^{(3)}]$ is negative in the frequency range of $\Delta_p \sim (1.3, 2.5)$, and the focusing effect takes place in this region; while $\mathrm{Re}[\chi_e^{(3)}]$ is positive in the range of $\Delta_p \sim (2.6, 3.1)$, and the defocusing effect occurs in this region. It is also seen that $\mathrm{Re}[\chi_e^{(3)}]$ can reach the order of 10^{-5}, one order higher than that of Ref. [17]. From Fig. 3(e), we also find that $\mathrm{Re}[\chi_e^{(3)}]$ is positive in the range of $\Delta_p \sim (4.1, 5.3)$, and the defocusing occurs in this region; then $\mathrm{Re}[\chi_e^{(3)}]$ is negative in the range of $\Delta_p \sim (5.4, 6)$, and the focusing effect occurs in this region. It can be found that the third-order nonlinearity is greatly enhanced to 10^{-4} and $\mathrm{Re}[\chi_e^{(3)}]/\mathrm{Re}[\chi_e^{(1)}]$ is about 10^{-15} [29] in the traditional medium. Therefore, the enhanced Kerr nonlinearity is realized in the multi left-handed frequency band, and maximum can be enhanced to 10^{-4} in

our scheme. Figures 3(b), 3(d), and 3(f) present the third-order nonlinear absorptions as a function of probe detuning in three left-handed frequency regions. It shows that $\mathrm{Im}[\chi_e^{(3)}]$ has different values in those three regions, and the magnitude of the imaginary part of $\chi_e^{(3)}$ increases as probe detuning increases. Although nonlinearity absorptions reach 10^{-7}, 10^{-5}, and 10^{-4} respectively (Figs. 3(b), 3(d), and 3(f))), compared with linear absorptions in those three frequency regions (Fig. 2(b)), the third-order absorption is much small. This left-handed atomic system can still maintain a low absorption.

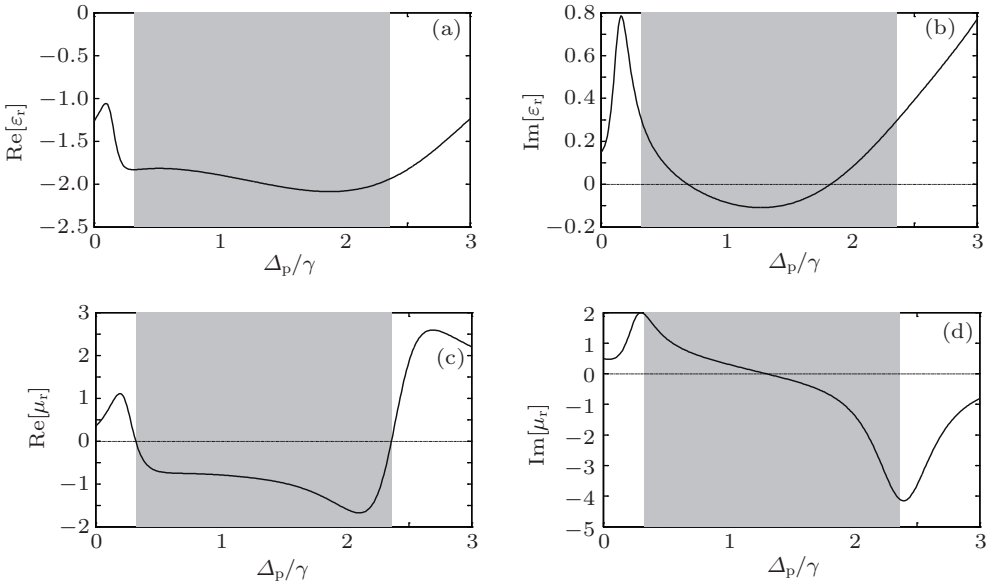


Fig. 4. Curves of real and imaginary parts of the permittivity ε_r (panels (a) and (b)), the permeability μ_r (panels (c) and (d)) versus Δ_p for the values of the bichromatic field: $\Omega_{c1} = \Omega_{c2} = \gamma$, δ=1.6γ. The left-handed properties are shown in gray regions.

Then we reduce both the Rabi frequencies of and frequency difference between the bichromatic fields, and analyze the electromagnetic properties of this atomic system under such a condition. The parameters of the bichromatic field will be adjusted as $\Omega_{c1} = \Omega_{c2} = \gamma$ and δ=1.6γ, other parameters remain unchanged. The electric response of the probe field is also very strong, the real part of the permittivity can realize fully negative in the detuning frequency range of $\Delta_p \sim (0,3)$ as shown in Fig. 4(a). However, the curve of the real part of the permeability has one negative band that is plotted in Fig. 4(b). As mentioned in Ref. [2] or other references, the permeability can obtain a negative value, owing to local field effect in a dense atomic system. Similarly, local field effect in our dense atomic system also plays a significant role in realizing negative permeability. From Fig. 4(c), we find that weakening the intensity of the bichromatic field and reducing the frequency difference of the bichromatic field will affect the permeability to achieve multi-peak negative values. Figures 4(c) and 4(d) show the imaginary parts of the permittivity and permeability. Figure 4(c) indicates a very low linear absorption in this left-handed frequency band, and a low gain absorption near the resonant frequency band. Figure 4(d) shows that the negative value of the imaginary part of the permeability increases gradually on the right side of the resonant frequency. As is well known, the absorption of a left-handed medium can be given by the expression $A = 2\pi Im(-\sqrt{\varepsilon\mu})$. Therefore, these phenomena will affect the absorption of a left-handed medium.

Figure 5(a) shows that the third-order nonlinearity $\mathrm{Re}[\chi_e^{(3)}]$ changes its sign twice in the left-handed range. At $\Delta_p \sim (0.3, 1.1)$ and $\Delta_p \sim (2.1, 2.38)$, the values of $\mathrm{Re}[\chi_e^{(3)}]$ are negative and the focusing occurs in these ranges, while at $\Delta_p \sim (1.2, 2)$, $\mathrm{Re}[\chi_e^{(3)}]$ is positive and the defocusing takes place in this band. The focusing and defocusing transformation are implemented in the different frequency intervals of the same left-handed frequency range. Compared with $\mathrm{Re}[\chi_e^{(3)}] \sim 10^{-6}$ in Ref. [17], in our system $\mathrm{Re}[\chi_e^{(3)}]$ can be enhanced by one order of magnitude as shown in Fig. 5(a). Figure 5(b) shows the curve of the third-order nonlinear absorption as a function of the probe detuning. The imaginary part of $\chi_e^{(3)}$ shows negative value in the frequency detuning range of $\Delta_p \sim (0.5, 1.5)$, and shows positive value in the range of $\Delta_p \sim (1.5, 2.3)$. $\mathrm{Im}[\chi_e^{(3)}]$ is about 4 orders smaller than $\mathrm{Im}[\varepsilon_r]$ (Fig. 4(b)) in the same frequency detuning range. The atomic system shows that the nonlinear absorption is quite small, the total absorption of this left-handed system can maintain a low value. Although the Kerr nonlinearity is not realized in the multi-band of left-handedness under such conditions, it has been achieved to transform effects twice in the same frequency band of the left-handed atomic system. This feature is similar to an optical switch. After varying the Rabi frequencies of and

frequency difference between the bichromatic fields, we also find that it can still be achieved to enhance Kerr nonlinearity in the weak probe field even by adjusting the parameters of the bichromatic field.

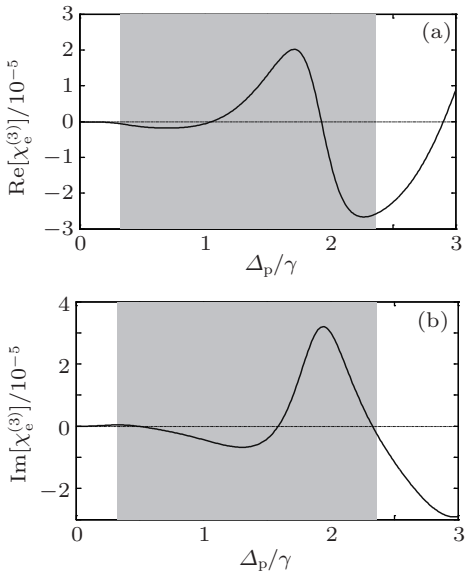


Fig. 5. Curves of real (a) and imaginary (b) parts of the third-order nonlinearity $\chi_e^{(3)}$ versus probe detuning Δ_p. for the left-handed atomic system in the gray region. The parameters are the same as those in Fig. 4.

4. Conclusion

In this paper, we investigate that left-handedness can be realized in the Λ-type three-level atomic system driven by a bichromatic field. Three frequency bands of left-handedness can be obtained in this atomic scheme via choosing appropriate parameters. In each frequency range of left-handedness, the third-order nonlinearity $\mathrm{Re}[\chi_e^{(3)}]$ has the focusing effect and the defocusing effect. Kerr nonlinearity is greatly enhanced in each left-handed frequency band. When we reduce the Rabi frequencies of and frequency difference between the bichromatic fields, the third-order nonlinearity $\mathrm{Re}[\chi_e^{(3)}]$ changes its sign twice in the same left-handed frequency band. We find that single-band or multi-band left-handed photonic resonant material can be realized by adjusting the parameters of the bichromatic field. Furthermore, the Kerr nonlinearity can be enhanced by an order of magnitude in a single-band atomic system and up to two orders of magnitude in a multi-band atomic system.

References

[1] Shelby R A, Smith D R and Schultz S 2001 *Science* **292** 77
[2] Pendry J B 2003 *Nature* **423** 22
[3] Parazzoli C G, Greegor R B, Li K, Koltenbah B E C and Tanielian M 2003 *Phys. Rev. Lett.* **90** 107401
[4] Cubukcu E, Aydin K, Ozbay E, Foteinopoulou S and Soukoulis C M 2003 *Nature* **423** 604
[5] Berrier A, Mulot M, Swillo M, Qiu M, Thylén L, Talneau A and Anand S 2004 *Phys. Rev. Lett.* **93** 073902
[6] Eleftheriades G V, Iyer A K and Kremer P C 2002 *IEEE Trans. Microw. Theory Tech.* **50** 2702
[7] Pendry J B 2004 *Science* **306** 1353
[8] Mackay T G and Lakhtakia A 2004 *Phys. Rev. E* **69** 026602
[9] Yannopapas V 2006 *J. Phys.: Condens. Matter* **18** 6883
[10] Oktel M Ö and Müstecaplioğlu Ö E 2004 *Phys. Rev. A* **70** 053806
[11] Shen J, Ruan Z and He S 2004 *J. Zhejiang Univ. Sci.* **5** 1322
[12] Thommen Q and Mandel P 2006 *Phys. Rev. Lett.* **96** 053601
[13] Zhang H, Niu Y and Gong S 2007 *Phys. Lett. A* **363** 497
[14] Ba N, Gao J, Fan W, Wang D, Ma Q, Wang R and Wu J 2008 *Opt. Commun.* **281** 5566
[15] Shen J Q 2006 *Phys. Lett. A* **357** 54
[16] Zhang H, Gong S, Niu Y, Li R X and Xu Z 2006 *Chin. Phys. Lett.* **23** 1769
[17] Zhao S C, Liu Z D and Wu Q X 2010 *Opt. Commun.* **283** 3301
[18] Kästel J and Fleischhauer M 2007 *Phys. Rev. Lett.* **98** 069301
[19] Zhao S C, Liu Z D and Wu Q X 2010 *J. Phys. B: At. Mol. Opt. Phys.* **43** 045505
[20] Yang X Y and Jiang Y Y 2012 *Opt. Commun.* **285** 2161
[21] Ficek Z and Freedhoff H S 1993 *Phys. Rev. A* **48** 3092
[22] Wang J, Zhu Y F, Jiang K J and Zhan M S 2003 *Phys. Rev. A* **68** 063810
[23] Hu X M, Xu Q, Li J Y, Li X X, Shi W X and Zhang X 2006 *Opt. Commun.* **260** 196
[24] Yang G Q, Xu P, Wang J, Zhu Y F and Zhan M S 2010 *Phys. Rev. A* **82** 045804
[25] Zhang H, Niu Y, Sun H and Gong S 2008 *Chin. Opt. Lett.* **6** 373
[26] Chu S I 1985 *Adv. At. Mol. Phys.* **21** 197
[27] Jackson J D 1999 *Classical Electrodynamics* (New York: John Wiley & Sons)
[28] Cook D M 1975 *The theory of the Electromagnetic Field* (New Jersey: Prentice-Hall)
[29] Boyd R W 1992 *Nonlinear Optics* (New York: Academic)
[30] Zhao S C, Liu Z D and Wu Q X 2010 *Chin. Phys. B* **19** 014211
[31] Zhang Z D, Liu Z D, Zhao S C, Zheng J, Ji Y F and Liu N 2011 *Chin. Phys. B* **12** 124202